The pyroptotic cell death effector Gasdermin D is activated by gout-associated uric acid crystals but is dispensable for cell death and IL-1β release

Maryam Rashidi[1,2], **Daniel S. Simpson**[1,2], **Anne Hempel**[3], **Daniel Frank**[1,2], **Emma Petrie**[1,2], **Angelina Vince**[1,2], **Rebecca Feltham**[1,2], **Jane Murphy**[1,2], **Simon M. Chatfield**[1,2], **Guy S. Salvesen**[3], **James M. Murphy**[1,2], **Ian P. Wicks**[1,2], **James E. Vince**[1,2,*]

[1]The Walter and Eliza Hall Institute of Medical Research, Parkville, VIC, 3052, Australia

[2]Department of Medical Biology, University of Melbourne, Parkville, VIC, 3010, Australia

[3]Sanford Burnham Prebys Medical Discovery Institute, La Jolla, CA, 92037, USA.

Abstract

The pyroptotic cell death effector, Gasdermin D (GSDMD), is required for murine models of hereditary inflammasome-driven, interleukin-1β (IL-1β)-dependent, autoinflammatory disease, making it an attractive therapeutic target. However, the importance of GSDMD for more common conditions mediated by pathological IL-1β activation, such as gout, remain unclear. In this study we address whether GSDMD, and the recently described GSDMD inhibitor, necrosulfonamide (NSA), contribute to Monosodium Urate (MSU) crystal-induced cell death, IL-1β release and autoinflammation. We demonstrate that MSU crystals, the aetiological agent of gout, rapidly activate GSDMD in murine macrophages. Despite this, the genetic deletion of GSDMD, or the other lytic effector implicated in MSU crystal killing, mixed lineage kinase domain-like (MLKL), did not prevent MSU crystal-induced cell death. Consequently, GSDMD or MLKL loss did not hinder MSU crystal-mediated release of bioactive IL-1β. Consistent with *in vitro* findings, IL-1β induction and autoinflammation in MSU crystal-induced peritonitis was not reduced in GSDMD deficient mice. Moreover, we show that the reported GSDMD inhibitor, NSA, blocks inflammasome priming and caspase-1 activation, thereby preventing pyroptosis independent of GSDMD targeting. The inhibition of cathepsins, widely implicated in particle-induced macrophage killing, also failed to prevent MSU crystal-mediated cell death. These findings i) demonstrate that not all IL-1β-driven autoinflammatory conditions will benefit from the therapeutic targeting of GSDMD, ii) document a unique mechanism of MSU crystal-induced macrophage cell death not rescued by pan-cathepsin inhibition, and iii) show that NSA inhibits inflammasomes upstream of GSDMD to prevent pyroptotic cell death and IL-1β release.

Introduction

Damaging environmental and host-derived particulate substances can elicit numerous inflammatory disorders, such as asbestosis, atherosclerosis, silicosis and osteoarthritis. Gout, one of the most common crystal-induced arthropathies, is a leading cause of inflammatory arthritis, and has also been associated with conditions such as the metabolic syndrome, renal disease and cardiovascular disease (1). Despite some advances in treatment strategies, there is no cure for gout and many patients experience recurrent flares that cause significant functional impairment and affect quality of life (2). There is evidence to suggest that distinct crystallopathies can share conserved biological mechanisms, such as the ability to activate proinflammatory inflammasome protein complexes and induce a necrotic-like, immune-modulatory, cell death (3). Therefore, a better understanding of the pathogenesis of gout-induced inflammation and cell death, and other particulate-mediated inflammatory conditions, will help guide the development of new therapeutics to improve patient outcomes.

Gout is characterized by the activation of inflammatory cascades that are caused by the precipitation of Monosodium Urate (MSU) in and around articular cavities. Animal models of gout and MSU crystal-driven inflammation implicate the caspase-1 activated cytokine, IL-1β, and consequently the IL-1 Receptor, as mediators of the MSU crystal-induced inflammatory response (4–8). These *in vitro* and murine studies have been confirmed by successful IL-1 inhibitor clinical trials (9, 10), although the expense of anti-IL-1 biologics, compared to traditional gout therapy, has to date limited wide-spread uptake.

IL-1β-driven autoinflammation results from the activation of intracellular multiprotein complexes known as inflammasomes (11). Inflammasome sensor proteins, including members of the NOD-like Receptor (NLR) family NLRP1, NLRP3 and NLRC4, the tripartite-motif family member Pyrin, and AIM2 (absent in myeloma 2), are innate immune cell pattern recognition receptors (PRRs). These cytosolic inflammasome PRRs specifically detect, and respond to, host- and pathogen-derived danger molecules to recruit and activate caspase-1, often via homotypic Caspase Activation and Recruitment Domain (CARD) interactions with the adaptor protein Apoptosis-associated Speck-like protein containing a CARD (ASC). Caspase-1 subsequently cleaves and thereby activates the cytokines IL-1β and IL-18, and also causes a lytic cell death, known as pyroptosis, to drive inflammatory responses. Of note, the NLRP3 inflammasome specifically senses inflammatory particulate matter, such as silica (12–14), alum (12, 15), cholesterol (16), amyloid-β (17) asbestos (13, 14), hydroxyapatite (18, 19) and MSU (4). Consequently, there is significant interest in defining how these potentially damaging particulate substances trigger NLRP3, IL-1β and cell death.

Studies have implicated particle phagocytosis, lysosomal membrane rupture, cathepsin activity and cellular potassium ion efflux as key events in their ability to initiate NLRP3 inflammasome signalling (12–18, 20–22). Imaging and chemical inhibitor studies also imply a similar, and possibly conserved, mechanism of particle-induced cell death, which has been reported to occur via particle-mediated lysosomal membrane rupture and be dependent on cathepsin activity (21, 23–26). However, attempts to genetically deplete cathepsins have

revealed either no, or only a minor, impact on particle-induced cell killing, with the addition of chemical pan-cathepsin inhibitors, such as high doses of CA-074 methyl ester (CA-074-Me), or K777, required for substantial protection (16, 21, 23, 27). Moreover, the ability of cathepsin inhibition to prevent macrophage cell death induced by MSU crystals has not been explored. Intriguingly, in neutrophils and kidney epithelial cells, it has been reported that several particles, such as calcium oxalate and MSU, induce programmed cell death via the necroptotic cell death machinery, Receptor Interacting Protein Kinase 3 (RIPK3) and its substrate, MLKL (28–30). This suggests that particles can elicit cell-type specific responses, or that distinct mechanisms of death occur in response to the type of particle.

The release of caspase-1 activated mature IL-1β into the extracellular milieu is also associated with necroptosis independent, caspase-1-mediated, pyroptotic killing, which can further contribute to inflammatory responses via the release of immunogenic cellular molecules (31, 32). Recently, it was discovered that caspase-1, and other inflammatory caspases such as caspase-11, induce pyroptosis by cleaving GSDMD to release an activated GSDMD N-domain that oligomerizes and forms pores in the plasma membrane (33–40). Consequently, in macrophages lacking GSDMD, not only is pyroptotic cell death ablated, but activated IL-1β accumulates in the cytosol, and its release is severely compromised (36–38). These studies indicate that GSDMD is required for the inflammation initiated by diverse inflammasome stimuli, such as nigericin activation of NLRP3, cytosolic LPS activation of caspase-11, bacterial toxin-induced activation of Pyrin and NLRC4, and DNA activation of the AIM2 inflammasome (36–38). Consistent with this idea, GSDMD loss prevents IL-1β responses following LPS injection *in vivo* (38) and, more recently, it was discovered that human disease-mimicking autoactivated Pyrin or NLRP3 mutant mice, and consequent sterile IL-1-driven autoinflammation, is rescued by GSDMD deficiency (41, 42). These findings lend weight to the idea that recently reported inhibitors of GSDMD (43, 44), may facilitate the development of novel drugs to target aberrant inflammasome and IL-1-driven inflammation. How beneficial GSDMD inhibition might be for the treatment of more widespread IL-1-driven autoinflammatory conditions, such as gout, has yet to be assessed, but is important for defining the scope, and potential benefit, of GSDMD targeted therapeutics. In this study we therefore sought to determine whether MSU crystals can activate GSDMD, and if so, how important GSDMD might be for MSU crystal-driven inflammation using gene targeted GSDMD mice and the recently described GSDMD inhibitor, necrosulfonamide (NSA) (43).

Materials and Methods

Antibodies and reagents

The primary antibodies used were against IL-1β (AF-401-NA, R&D), caspase-1 (AG-20B-0042-C100, Adipogene), GSDMD (ab210070, Abcam), MLKL (generated in house (74), available from Millipore, MABC604, clone 3H1) and β-actin (A-1978, Sigma-Aldrich). Flow cytometric staining utilized the following antibodies from BioLegend; purified anti-mouse CD16/32 antibody (101302), APC-conjugated anti-Ly6G (127614), FITC-conjugated anti-F4/80 (123108), PE-conjugated anti-B220 (103208), APC-CY7-conjugated anti-CD3 (100222) and Brilliant Violet 421-conjugated anti-CD11b (101236).

123 count eBeads were purchased from Thermo scientific (01-1234-42). Ultrapure LPS (tlrl-smlps) and nigericin (tlrl-nig) were purchased from InvivoGen. MSU was generated in house, as previously described(63, 75). Imject™ Alum Adjuvant (77161, thermo scientific), Z-VAD-fmk (187389-52-2, Santa Cruz Biotechnology), CA-074-Me (sc-214647, Santa Cruz Biotechnology), necrosulfonamide (ab143839, Abcam), potassium chloride (P954, Sigma-Aldrich) and glycine (G7126; Sigma-Aldrich) were purchased as indicated.

Cell culture

Bone marrow-derived macrophages (BMDMs) were generated from WT C57BL/6, *Gsdmd*$^{-/-}$, *Caspase-1*$^{-/-}$ and *Mlkl*$^{-/-}$ mice (aged 8–12 weeks). The *Gsdmd*$^{-/-}$ (38), *Caspase-1*$^{-/-}$ (76)(also harbouring an inactivating caspase-11 mutation) and *Mlkl*$^{-/-}$ (74) mice were either generated on a C57BL/6 background (*Mlkl*$^{-/-}$, *Gsdmd*$^{-/-}$), or backcrossed for 10 generations or more (*Caspase-1*$^{-/-}$). Cells from tibiae and femora were cultured in DME, 10% FCS (Sigma-Aldrich) and 20% L929 conditioned-medium (in-house, WEHI) at 37°C in a 10% CO_2 incubator. After 6 days, adherent cells were harvested and seeded at a density of 1.5×10^5 in 200 μl of medium in replicates, in flat-bottom 96-well plates. Following overnight rest, the medium was changed and cells were primed with ultrapure LPS (50 ng/ml) for 2.5 h and then exposed to the indicated concentrations of MSU, alum and nigericin. Supernatant was collected after 1 h of Nigericin exposure or 6 h of MSU or alum exposure for further analysis.

Cytokine ELISAs

Levels of IL-1β (#DY401, R&D Systems), TNF (#5017331, eBioscience) and IL-6 (#5017219, eBioscience) were assayed by ELISA according to instructions of the manufacturer.

LDH assay

LDH release into the cell supernatants was measured with a 30-minute coupled enzymatic assay, using the CytoTox 96 Non-Radioactive Cytotoxicity Assay kit according to the manufacturer's instructions (#G1780, Promega).

Immunoblot analysis

BMDM cell lysates and supernatants (reduced and denatured) were fractionated by sodium dodecyl sulphate-polyacrylamide gel electrophoresis (SDS-PAGE) (4–20% NuPAGE gels, Invitrogen). Proteins were then electrophoretically transferred to nitrocellulose membranes and blocked in 5% w/v skim milk in PBS containing 0.1% Tween20 (SM-PBST) prior to incubation with primary antibody (diluted 1:1000 in SM-PBST, unless stated otherwise) overnight at 4 °C. Following 4–5 washes for 5 min each in PBST, membranes were incubated with HRP-conjugated secondary antibody (diluted in SM-PBST) for 1–2 hours at room temperature. Membranes were then washed 4–5 times for 5 min each in PBST and proteins of interested detected by enhanced chemiluminescence (ECL) and an X-OMAT developer (Kodas), or the ChemiDoc Touch Imaging System (Bio-Rad) and Image Lab Software.

Flowcytometry analysis

Peritoneal cells were incubated with anti-mouse CD16/32 antibody and fluorescent-conjugated antibodies in round-bottom polystyrene tubes for 15 min on ice in 50 μl of cold FACS buffer (PBS, 2% FCS, 2 mM EDTA) at the concentrations indicated by the manufacturer (BioLegend); APC-conjugated anti-Ly6G, FITC-conjugated anti-F4/80, PE-conjugated anti-B220, APC-CY7-conjugated anti-CD3, Brilliant Violet 421-conjugated anti-CD11b. Propidium iodide staining was used to exclude dead cells and 123count eBeads Counting Beads were used for absolute counting of cells (Thermo Scientific). Cells were analyzed via a FACSVerse flow cytometer (BD Biosciences).

MSU crystal injections

The indicated (figure legends) female or male C57BL/6, *Caspase-1*$^{-/-}$ and *Gsdmd*$^{-/-}$ mice aged 8–12 weeks were injected with MSU crystals (3 or 5 mg i.p.) or carrier (PBS). After 4 h, mice were culled by CO2-induced asphyxia. Peritoneal lavages were performed using 1.5 ml of PBS containing 5mM EDTA. The peritoneal fluid was spun down and the supernatant were collected for measurement of cytokines by ELISA. Cells were identified by antibody staining (neutrophils: CD11b$^+$, Ly6G$^+$, Monocytes: CD11b$^+$, Ly6G$^-$, macrophages: CD11b$^+$, F4/80$^+$ upon exclusion of T cells (CD3$^+$), B-cells (B220$^+$) and dead cells (PI$^+$)) and analyzed by flow cytometry.

Imaging

BMDMs were seeded at 4×10^5 cells in a 24 well tissue culture plates and stimulated as indicated in the figure legends. Cells were then stained with propidium iodide (PI, 8 μg/ml) and imaged using an Olympus IX70 florescent microscope and cellSens Standard software. Quantification of PI staining was performed using Fiji software.

Results

MSU crystals activate GSDMD, but GSDMD is dispensable for MSU crystal-induced IL-1β release and cell death in vitro

Consistent with past research (4, 12), the stimulation of LPS primed bone marrow derived macrophages (BMDMs) with alum particles or MSU crystals for 1.5–6 hours resulted in significant activation and secretion of caspase-1 and IL-1β as reflected by processing to their p20 and p17 fragments, respectively, and their release into the cell supernatant (Fig. 1A). In parallel with these events, within 1.5 hours of MSU crystal or alum treatment, we detected cleavage of GSDMD into its active p30, pore-forming, N-domain in both the cell lysate and cell supernatant (Fig. 1A), suggesting that GSDMD may contribute to MSU crystal-dependent IL-1β release and/or cell death.

It was initially reported that after 16 hours of MSU crystal treatment, IL-1β release (as measured by ELISA) was not different between wildtype (WT) and GSDMD deficient cells (38). However, as demonstrated in Fig. 1, particulate NLRP3 activators, such as MSU, can engage caspase-1 to activate GSDMD and IL-1β within 1.5 hours. Moreover, NLRP3 stimuli that initially release IL-1β in a GSDMD-dependent manner, such as ATP and nigericin, undergo a secondary mode of cell death that allows GSDMD-independent IL-1β release

upon prolonged treatment (36–38, 45, 46). Therefore, as recently highlighted (5), whether GSDMD might participate in MSU crystal-generated inflammation and cell death remains unclear.

To genetically define if MSU crystal-activated GSDMD contributes to MSU crystal-induced IL-1β release, or cell death, we primed wildtype (WT), *Gsdmd*^−/− and *Caspase-1*^−/− BMDMs with LPS and then exposed cells to increasing concentrations of MSU crystals, alum particles or the soluble NLRP3 activator, nigericin. As expected, compared to WT macrophages, IL-1β release after 1 hour of nigericin treatment was blocked in both caspase-1 and GSDMD deficient BMDMs (Fig. 1B), although TNF secretion was not impacted (Fig. 1C). In contrast, although IL-1β release following MSU crystal or alum treatment was abrogated in caspase-1 deficient BMDMs when compared to WT cells, it was not altered upon deletion of GSDMD at any time point examined, from 1.5 to 6 hours (Fig. 1B and Fig. S1A). The genetic deletion of Caspase-1 or GSDMD also had no impact on TNF secretion upon particle stimulation (Fig. 1C and Fig. S1A).

To directly measure the impact of GSDMD loss on MSU crystal-induced NLRP3 responses, we examined caspase-1 and IL-1β cleavage by Western blot. Unlike ELISA analysis that detects both inactive precursor and mature IL-1β (47), Western blotting provides a direct measure of both caspase-1 and IL-1β cleavage, and hence, activation status. Consistent with our ELISA data, MSU crystal-induced caspase-1 cleavage and IL-1β maturation and release was comparable between WT and GSDMD deficient BMDMs, but was undetectable upon caspase-1 loss (Fig. 1D). On the other hand, caspase-1 and GSDMD were both required for efficient release of nigericin activated IL-1β, although at higher nigericin concentrations some GSDMD-independent IL-1β release was detected (Fig. S1B).

Because GSDMD-induced cell death can, in some circumstances, be separated from GSDMD-dependent IL-1β secretion (45, 48), we next examined if GSDMD might contribute to MSU crystal or alum particle killing. However, MSU crystal- or alum-induced cell death, as measured by propidium iodide uptake and fluorescence microscopy (Fig. 2A, 2B), or cellular LDH release (Fig. 2C), was not impacted by GSDMD or caspase-1 loss at any time point, or any particle concentration, examined. In contrast, caspase-1 or GSDMD deletion prevented nigericin-induced cell death after 1 hour of treatment, while after 5 hours of stimulation *Gsdmd*^−/− BMDMs also succumbed to nigericin killing (Fig. 2A–2C).

Therefore, although MSU crystals can induce a robust caspase-1 and GSDMD activation response within 1.5 hours of stimulation, the ability of MSU crystals to induce cell death and trigger IL-1β release *in vitro* is not dependent on GSDMD.

Necrosulfonamide, a recently described GSDMD inhibitor, blocks inflammasome-mediated caspase-1 activation to limit MSU crystal and nigericin induced IL-1β release

Necrosulfonamide (NSA) was initially identified as binding to cysteine 86 of human MLKL to inhibit MLKL-mediated necroptotic cell death (49). Recently, Rathkey *et al.*, reported that NSA also inhibits processed GSDMD activity by binding cysteine 191 to block GSDMD N-domain oligomerization and pore formation, and NSA thereby limits IL-1β release and pyroptotic killing, but not GSDMD cleavage (43). Consequently, we reasoned that NSA

should not limit MSU crystal- or nigericin-mediated caspase-1 processing, or intracellular IL-1β maturation to its active p17 fragment, as all of these events occur upstream, and independent of, GSDMD.

Unexpectedly, particularly in view of our data demonstrating that MSU crystal-mediated IL-1β release is GSDMD-independent (Fig. 1 and Fig. S1), the treatment of LPS primed BMDMs with similar concentrations of NSA used by Rathkey *et al.,* (1–10 μM) efficiently inhibited MSU crystal-induced IL-1β release in a dose dependent manner, akin to its ability to limit nigericin-mediated IL-1β release (Fig. 3A, 3B). On the other hand, MSU crystal-mediated cell death was not altered by NSA treatment in either WT or MLKL deficient macrophages, whereas NSA efficiently blocked nigericin killing (Fig. 3A, 3B, Fig. S2A and Fig. S3C).

Further examination by Western blotting revealed that NSA efficiently prevented ATP, nigericin- and MSU crystal-induced caspase-1 processing and, consequently, cleavage and activation of IL-1β (Fig. 3C, 3D, Fig. S2B, S2C and Fig. S3B). Moreover, consistent with our data documenting NSA-mediated blockade of caspase-1 activation, we observed that NSA inhibited GSDMD processing to the active N-terminal p30 domain (Fig. 3C, 3D and Fig. S2B). Importantly, NSA effectively blocked the accumulation of intracellular processed caspase-1 and IL-1β that occurs upon GSDMD deletion, thereby demonstrating that NSA must inhibit inflammasome activity independent of GSDMD (Fig. 3C and Fig. S2B). Consistent with this, we observed that NSA also limited nigericin-induced ASC speck formation, which is required for proximity-induced caspase-1 activation (Fig. 3E). Interestingly, NSA potently blocked IL-1β precursor production upon LPS stimulation (Fig. S2D), suggesting it can limit IL-1β activation, at least in part, by reducing LPS-induced gene transcription. Collectively, these data demonstrate that the impact of NSA on inflammasome activity and pyroptosis can occur independent of its ability to target GSDMD.

MSU crystal-induced cell death does not require the necroptotic effector MLKL

Necroptotic, membrane-associated, MLKL causes potassium ion efflux to induce cell intrinsic NLRP3 inflammasome activation and IL-1β secretion, independent of GSDMD (50). MLKL-induced cellular responses thereby resemble MSU-crystal stimulation, with both activating NLRP3 in a potassium efflux dependent manner and inducing cell death and IL-1β release independent of GSDMD. In fact, it has been reported that MSU crystal-induced kidney and neutrophil cell death requires MLKL (28–30, 51), the first reported target of NSA (49). Therefore, we considered if MSU crystal-mediated macrophage killing or NLRP3 activation requires MLKL. We exposed WT and MLKL-deficient BMDMs to MSU crystals or nigericin in the presence or absence of the pan-caspase inhibitors, Z-VAD-fmk or IDN-6556. Both MSU crystal- and nigericin-induced cell death, as well as caspase-1 and IL-1β processing and release, were unaffected by the loss of MLKL when compared to WT cells (Fig. 4A–D). As expected, treatment of LPS primed WT or *Mlkl*⁻/⁻ BMDMs with Z-VAD-fmk or IDN-6556 to inhibit caspase activity prevented both nigericin- and MSU-induced caspase-1 cleavage to its p20 subunit, limited GSDMD processing, and blocked IL-1β maturation and release (Fig. 4D and S3A). However, MSU crystals did not trigger significant caspase-8 or caspase-3 activation (Fig. S3A), and pan-caspase inhibition had no

impact on MSU crystal-induced cell death in either WT or *Mlkl*^{−/−} macrophages (Fig. 4C). As expected, LPS and Smac-mimetic, or LPS and caspase inhibitor, co-treatment induced caspase- and MLKL-dependent cell death, respectively (Fig. 4C). Therefore, in macrophages, the combined loss of MLKL-mediated necroptosis and caspase-dependent cell death modalities (i.e. apoptosis and pyroptosis) do not inhibit MSU crystal-mediated killing, and MLKL is not required for MSU crystal-induced NLRP3 inflammasome activation.

MSU crystal-induced cellular rupture is not significantly protected by the osmoprotectant glycine, inhibition of cellular cathepsins, or the prevention of potassium ion efflux

Our data, and those of others (52), support the idea that particle-induced loss of plasma membrane integrity is required for mature IL-1β release. Both pyroptotic (53) and necroptotic (50) induced lytic membrane rupture is delayed by the osmoprotectant glycine, and this consequently limits the release of intracellular proteins such as LDH, but does not impact mature IL-1β secretion. However, in contrast to the membrane-protective effect of glycine on these lytic cell death modalities, glycine failed to limit MSU crystal-induced LDH release (Fig. 5A). As expected, glycine did afford significant protection from nigericin-induced pyroptotic membrane rupture (Fig. 5A), but had no impact on either MSU crystal- or nigericin-induced caspase-1 and GSDMD processing, or IL-1β maturation (Fig. 5B, 5C and 5D). Similarly, increasing extracellular potassium chloride levels to prevent potassium ion efflux, like glycine treatment, had no effect on MSU crystal-induced LDH release in either WT, *Gsdmd*^{−/−} or *Caspase-1*^{−/−} BMDMs, despite effectively blocking NLRP3 inflammasome pyroptotic killing by nigericin (Fig. 5A). This finding contrasted with the ability of increased extracellular potassium chloride to inhibit both MSU crystal- and nigericin-mediated caspase-1, GSDMD and IL-1β processing (Fig. 5B, 5C and 5D). Therefore, although potassium ion efflux is a common denominator by which MSU crystals, MLKL, and GSDMD trigger NLRP3 activation, MSU crystal-induced cellular rupture is distinct from glycine-inhibited pyroptotic- and necroptotic-associated membrane lysis.

The current paradigm argues that particulate NLRP3 activators are phagocytosed by macrophages to rupture lysosomal membranes, and that this triggers cathepsin release into the cytosol and cathepsin-dependent NLRP3 signaling and cell death (54). The cathepsin B inhibitor CA-074-Me efficiently targets multiple cathepsins at concentrations greater than 1 μM (20), and at 10–20 μM it can inhibit lysosomal-induced cell death, similar to the inhibition of particle killing by 10–20 μM treatment with K777, another pan-cathepsin inhibitor (21). Surprisingly however, we observed that the levels of cell death, as measured by LDH release or propidium iodide uptake, in BMDMs treated with 20–40 μM CA-074-Me and then stimulated with MSU crystals, was only marginally reduced compared to control MSU crystal-treated cells, even when CA-074-Me was used at 40 μM on a GSDMD or caspase-1 deficient background (Fig. 5A, 6A and Fig. S4A). This was despite the fact that 40 μM of CA-074-Me limited nigericin-induced pyroptosis, and also inhibited alum-mediated cell death (Fig. 5A, 6A and Fig. S4A). Moreover, at doses up to 40 μM, the pan-cathepsin inhibitor K777 failed to reduce MSU crystal-mediated macrophage death, even though K777 limited alum-dependent cell killing and blocked alum-induced NLRP3 inflammasome responses (Fig. 6A, 6B, 6C and Fig. S4A). Overall, these data show that pan-cathepsin inhibition does not abrogate MSU crystal-mediated macrophage cell death.

Although CA-074-Me did not greatly impact MSU crystal-induced macrophage killing, 20–40 μM of CA-074-Me abrogated MSU crystal-induced caspase-1, GSDMD and IL-1β processing and release, and also inhibited nigericin-mediated NLRP3 responses in a dose dependent manner (Fig. 5B, 5C and 6A and Fig. S4A). Therefore, although CA-074-Me does not efficiently block MSU crystal-dependent macrophage death, it targets a pathway that is required for the activation of NLRP3 by both particulate and soluble stimuli. The impact of K777 on MSU crystal-induced NLRP3 and IL-1β activation was less clear because it dramatically reduced cellular precursor IL-1β levels (Fig. 6C, 6D), consistent with evidence that it, and to a lesser extent CA-074-Me, can inhibit inflammasome priming (Fig. 6D)(20).

In vivo MSU-induced inflammation and IL-1β production does not require GSDMD

To test whether GSDMD is required for MSU crystal-induced inflammatory responses *in vivo*, WT (C57BL/6) and GSDMD deficient mice were injected intraperitoneally with MSU crystals (3 mg or 5 mg), or carrier (PBS) control. After 4 hours mice were culled and their peritoneal cells and fluid analyzed for neutrophil and monocyte influx, and cytokine levels, respectively.

MSU crystal injection resulted in similar increases in both IL-1β and IL-6 in the peritoneal fluid of WT and GSDMD deficient mice when compared to carrier control treated animals (Fig. 7A and 7B). Consistent with no difference in the levels of these inflammatory cytokines, MSU crystal-induced neutrophil and monocyte infiltration into the peritoneal cavity did not differ between WT and *Gsdmd*$^{-/-}$ animals (Fig. 7C and 7D). The injection of MSU crystals into caspase-1 deficient animals also did not significantly impact cytokine levels or neutrophil and monocyte infiltration into the peritoneal fluid when compared to WT control animals (Fig. S4B and S4C). Therefore, caspase-1 and GSDMD are not essential for MSU crystal-induced autoinflammation *in vivo*.

Discussion

MSU crystals drive autoinflammation in gout through the activation of IL-1β and cell death (5). The inflammasome sensor, NLRP3, and its downstream signaling components, ASC, Caspase-1, IL-1β and the IL-1R, have all been reported to contribute to MSU crystal-driven inflammation, both *in vitro* and, albeit to varying extents, *in vivo* (4–8, 55–59). However, as recently highlighted (5), whether activated GSDMD participates in MSU crystal-generated IL-1β release and inflammation has not been established. Here we demonstrate a number of important features of cellular MSU crystal-induced responses that distinguish it from other IL-1β-driven, autoinflammatory, diseases. First, although MSU crystals rapidly activate GSDMD, GSDMD is dispensable for MSU crystal-mediated inflammation and cell death, both *in vitro* and *in vivo*. Despite this, the recently reported GSDMD inhibitor, NSA (43), still efficiently limits MSU crystal activation of caspase-1 and IL-1β, indicating NSA blocks inflammasome signaling upstream of GSDMD. Second, the necroptotic lytic cell death effector MLKL is not required for MSU-crystal induced death or NLRP3 activation in macrophages, which contrasts with the reported role for MLKL in MSU crystal-mediated death of other cell types (28–30, 51). Third, cathepsin inhibition, or the blockade of

potassium ion efflux, despite preventing MSU crystal- and nigericin-mediated NLRP3 inflammasome responses, had no significant impact on MSU crystal-induced killing.

GSDMD pores are important for IL-1β release and pyroptotic cell death following the activation of numerous inflammasomes, such as NLRP3, NLRC4, Pyrin, AIM2, and the non-canonical caspase-11 inflammasome (36, 38). However, prolonged NLRP3 and AIM2 stimulation can also result in GSDMD-independent cell death and IL-1β release (36–38, 45, 46). Nevertheless, the importance of GSDMD for autoactivating NLRP3 and Pyrin mutant, IL-1β-driven, disease *in vivo* has recently been established (41, 42). These observations highlight the need to assess the role of GSDMD in other IL-1-dependent inflammatory conditions. In this regard, our data suggest that targeting GSDMD would not be therapeutically beneficial in alleviating gout-associated inflammation nor, most likely, other crystallopathies (60). Interestingly, we also show that *in vivo* administration of MSU crystals induces peritoneal IL-1β production and inflammatory cell infiltration independent of caspase-1, in agreement with the idea that other enzymes, particularly *in vivo*, can significantly contribute to IL-1β activation and the ensuing inflammatory response (57). While it has been reported that caspase-1 deficiency partially reduces *in vivo* MSU crystal responses (7, 56, 58), differences in the amount of MSU crystals used, their route of administration (e.g. intraarticular versus intraperitoneal), the time points examined, and the tissue types sampled, may all explain variable results.

Despite GSDMD being dispensable for MSU crystal-induced death and IL-1β release, both MSU crystals and alum particles rapidly activate GSDMD. We have recently shown that Bax and Bak mediated mitochondrial apoptotic signaling can engage caspase-1 to cleave GSDMD yet, akin to MSU crystals, GSDMD is also not required for Bax and Bak-driven cell death or IL-1β release (61). Similarly, the necroptotic effector MLKL can trigger NLRP3 and IL-1β release independent of GSDMD (50, 62). In all these scenarios, it is likely that GSDMD-independent membrane damage and potassium ion efflux is requisite for NLRP3 activation and, consequently, GSDMD will be activated after the terminal damage to cellular membranes has already been initiated. This model is consistent with our observations here, and other reports (14, 15, 21, 23, 60), demonstrating that particulate induced macrophage killing occurs independent of potassium ion efflux, NLRP3 inflammasome formation, and caspase-1 activity. However, the robust MSU crystal and alum activation of GSDMD we observed raises the theoretical possibility that GSDMD may contribute to particulate inflammatory responses under different conditions. For example, in cell types that cannot readily engage the canonical MSU crystal-induced cell death pathway, GSDMD-dependent death may become dominant. Although some controversy exists (63), it is interesting to note that in neutrophils and kidney cells MSU crystals have been reported to engage the necroptotic effector MLKL to induce cell death (28–30, 51). While our genetic data show that MLKL is not required for macrophage cell death or NLRP3 inflammasome responses elicited by MSU crystal stimulation, this serves to highlight the potential for cell-type specific responses to inflammatory particles.

The unique killing mechanism by which MSU-crystals induce macrophage cell death is emphasized by our findings demonstrating that i) unlike pyroptosis (64, 65) and necroptosis (50), the osmoprotectant glycine does not limit MSU crystal-induced cellular rupture and ii),

MSU-crystal killing is not significantly reduced by cathepsin inhibition. The later observation is surprising given that numerous studies have utilized CA-074-Me (12, 17, 18, 21), or K777 (21), to block cathepsin activity and inhibit particle-induced macrophage responses. However, to our knowledge, the impact of these cathepsin inhibitors on MSU crystal-dependent macrophage death has not been examined. The doses of cathepsin inhibitor we used (up to 40 μM) exceed those (10–20 μM) that have been demonstrated to inhibit cell death and/or inflammasome activity mediated by other particulate NLRP3 activators (12, 18, 21, 22). Although high dose CA-074-Me afforded a small degree of protection against MSU crystal killing, it remains to be determined whether this represents specific CA-074-Me inhibition of cathepsin activity or off-target effects. Unlike cell impermeable CA-074, CA-074-Me has dramatically reduced specificity for cathepsin B, inhibits multiple cathepsins, and targets a number of proteins of undetermined identity, possibly upstream of lysosomal disruption (66, 67). The potential off-target impact of CA-074-Me is emphasized by its ability to inhibit diverse cellular functions, such as necroptotic cell death (68), apoptotic killing (69), and ATP and nigericin induced NLRP3 activation and pyroptosis (24, 70). Hence, given the potential unreliability of CA-074-Me, and that high dose K777, a pan-cathepsin inhibitor, afforded no protection to MSU crystal macrophage killing, we conclude that cathepsin activity is unlikely to be essential for MSU crystal killing. We suggest that irreversible particle-induced lysosomal membrane rupture, reported to occur independent of cathepsin activity (23, 24), defines the point of no return for MSU crystal-mediated macrophage killing. Hence, although cathepsin inhibition may delay cell death for some particulate stimuli, ultimately it will not prevent it. This concept is similar to that demonstrated for mitochondrial apoptosis, whereby Bax/Bak-mediated disruption to mitochondrial membrane integrity suffices to induce cell death, even when the apoptosome caspase-activating complex, which forms in response to the release of mitochondrial cytochrome c, is eliminated (71, 72).

Whether lysosomal cathepsin activity is required for MSU crystal-dependent NLRP3 activation requires more detailed experimentation. Although CA-074-Me efficiently blocked MSU crystal activation of caspase-1 and IL-1β it has likely off-target effects at the doses required to inhibit NLRP3. Our data also demonstrates that the pan-cathepsin inhibitor K777, and to a lesser extent CA-074-Me, dramatically blunts LPS-induced IL-1β and NLRP3 protein production to prevent inflammasome priming, likely at the level gene transcription (20). Genetic deletion of cathepsin B, C and S combined with siRNA targeting of cathepsins X and L, only results in, at best, a minor loss to silica-induced IL-1β secretion. While compensatory upregulation of cathepsin activity and/or redundancy has been suggested to account for the inability of genetic experiments to pin down a conclusive role for specific cathepsins in activating NLRP3 (20), cathepsin substrates that trigger potassium ion efflux to activate NLRP3 remain unknown. Interestingly, however, unlike other particulate NLRP3 activators (16, 22), the inhibition of lysosomal function with Bafilomycin A1 has been reported to have no impact on MSU crystal-induced IL-1β maturation and release (27)(our data not shown). Evidence indicates that particles, such as alum (73) and MSU (25, 73), can engage membrane lipids to trigger damage and/or phagocytic pathways, and that cholesterol crystal-induced disruption of plasma membrane homeostasis may directly precipitate cell death (60). These findings need to be reconciled with other studies

suggesting that cholesterol crystals disrupt lysosomes and require cathepsin activity for NLRP3 signaling and cell killing (16, 21). Similarly, despite reports implicating lysosomal rupture and cathepsin function in alum-induced NLRP3 inflammasome activation (12, 15), alum has been suggested to activate IL-1β in dendritic cells through plasma membrane lipid engagement without internalization (73). Clearly, more research is required to clarify how particulate inflammatory mediators trigger cell death and inflammation to cause disease. We suggest that differences in the modality of particle-mediated cell death and in IL-1β activating mechanisms vary, depending on both the type and size of particle, and on the nature of the responding cell. Nevertheless, our findings document a unique mode of macrophage cell death induced by MSU crystals and demonstrate that therapeutic targeting of GSDMD is unlikely to be uniformly beneficial for IL-1β-associated autoinflammatory conditions.

Supplementary Material

Refer to Web version on PubMed Central for supplementary material.

Acknowledgments:

References

1. Kuo CF, Grainge MJ, Zhang W, and Doherty M. 2015 Global epidemiology of gout: prevalence, incidence and risk factors. Nat Rev Rheumatol 11: 649–662. [PubMed: 26150127]

2. Edwards NL 2011 Quality of care in patients with gout: why is management suboptimal and what can be done about it? Curr Rheumatol Rep 13: 154–159. [PubMed: 21161617]

3. Mulay SR, and Anders HJ. 2016 Crystallopathies. N Engl J Med 374: 2465–2476. [PubMed: 27332905]

4. Martinon F, Pétrilli V, Mayor A, Tardivel A, and Tschopp J. 2006 Gout-associated uric acid crystals activate the NALP3 inflammasome. Nature 440: 237–241. [PubMed: 16407889]

5. So AK, and Martinon F. 2017 Inflammation in gout: mechanisms and therapeutic targets. Nat Rev Rheumatol 13: 639–647. [PubMed: 28959043]

6. Chen CJ, Shi Y, Hearn A, Fitzgerald K, Golenbock D, Reed G, Akira S, and Rock KL. 2006 MyD88-dependent IL-1 receptor signaling is essential for gouty inflammation stimulated by monosodium urate crystals. J Clin Invest 116: 2262–2271. [PubMed: 16886064]

7. Reber LL, Marichal T, Sokolove J, Starkl P, Gaudenzio N, Iwakura Y, Karasuyama H, Schwartz LB, Robinson WH, Tsai M, and Galli SJ. 2014 Contribution of mast cell-derived interleukin-1beta to

uric acid crystal-induced acute arthritis in mice. Arthritis & rheumatology (Hoboken, N.J.) 66: 2881–2891.

8. Gross O, Yazdi AS, Thomas CJ, Masin M, Heinz LX, Guarda G, Quadroni M, Drexler SK, and Tschopp J. 2012 Inflammasome activators induce interleukin-1alpha secretion via distinct pathways with differential requirement for the protease function of caspase-1. Immunity 36: 388–400. [PubMed: 22444631]

9. So A, De Meulemeester M, Pikhlak A, Yucel AE, Richard D, Murphy V, Arulmani U, Sallstig P, and Schlesinger N. 2010 Canakinumab for the treatment of acute flares in difficult-to-treat gouty arthritis: Results of a multicenter, phase II, dose-ranging study. Arthritis Rheum 62: 3064–3076. [PubMed: 20533546]

10. Sivera F, Wechalekar MD, Andres M, Buchbinder R, and Carmona L. 2014 Interleukin-1 inhibitors for acute gout. Cochrane Database Syst Rev: CD009993.

11. Schroder K, and Tschopp J. 2010 The inflammasomes. Cell 140: 821–832. [PubMed: 20303873]

12. Hornung V, Bauernfeind F, Halle A, Samstad EO, Kono H, Rock KL, Fitzgerald KA, and Latz E. 2008 Silica crystals and aluminum salts activate the NALP3 inflammasome through phagosomal destabilization. Nat Immunol 9: 847–856. [PubMed: 18604214]

13. Dostert C, Pétrilli V, Van Bruggen R, Steele C, Mossman BT, and Tschopp J. 2008 Innate immune activation through Nalp3 inflammasome sensing of asbestos and silica. Science 320: 674–677. [PubMed: 18403674]

14. Cassel SL, Eisenbarth SC, Iyer SS, Sadler JJ, Colegio OR, Tephly LA, Carter AB, Rothman PB, Flavell RA, and Sutterwala FS. 2008 The Nalp3 inflammasome is essential for the development of silicosis. Proc Natl Acad Sci U S A 105: 9035–9040. [PubMed: 18577586]

15. Eisenbarth SC, Colegio OR, O'Connor W, Sutterwala FS, and Flavell RA. 2008 Crucial role for the Nalp3 inflammasome in the immunostimulatory properties of aluminium adjuvants. Nature 453: 1122–1126. [PubMed: 18496530]

16. Duewell P, Kono H, Rayner KJ, Sirois CM, Vladimer G, Bauernfeind FG, Abela GS, Franchi L, Nunez G, Schnurr M, Espevik T, Lien E, Fitzgerald KA, Rock KL, Moore KJ, Wright SD, Hornung V, and Latz E. 2010 NLRP3 inflammasomes are required for atherogenesis and activated by cholesterol crystals. Nature. 464: 1357–1361. [PubMed: 20428172]

17. Halle A, Hornung V, Petzold GC, Stewart CR, Monks BG, Reinheckel T, Fitzgerald KA, Latz E, Moore KJ, and Golenbock DT. 2008 The NALP3 inflammasome is involved in the innate immune response to amyloid-beta. Nat Immunol 9: 857–865. [PubMed: 18604209]

18. Jin C, Frayssinet P, Pelker R, Cwirka D, Hu B, Vignery A, Eisenbarth SC, and Flavell RA. 2011 NLRP3 inflammasome plays a critical role in the pathogenesis of hydroxyapatite-associated arthropathy. Proc Natl Acad Sci U S A 108: 14867–14872. [PubMed: 21856950]

19. Pazar B, Ea HK, Narayan S, Kolly L, Bagnoud N, Chobaz V, Roger T, Liote F, So A, and Busso N. 2011 Basic calcium phosphate crystals induce monocyte/macrophage IL-1beta secretion through the NLRP3 inflammasome in vitro. J Immunol 186: 2495–2502. [PubMed: 21239716]

20. Orlowski GM, Colbert JD, Sharma S, Bogyo M, Robertson SA, and Rock KL. 2015 Multiple Cathepsins Promote Pro-IL-1beta Synthesis and NLRP3-Mediated IL-1betaActivation. J Immunol 195: 1685–1697. [PubMed: 26195813]

21. Orlowski GM, Sharma S, Colbert JD, Bogyo M, Robertson SA, Kataoka H, Chan FK, and Rock KL. 2017 Frontline Science: Multiple cathepsins promote inflammasome-independent, particle-induced cell death during NLRP3-dependent IL-1beta activation. J Leukoc Biol 102: 7–17. [PubMed: 28087651]

22. Munoz-Planillo R, Kuffa P, Martinez-Colon G, Smith BL, Rajendiran TM, and Nunez G. 2013 K(+) efflux is the common trigger of NLRP3 inflammasome activation by bacterial toxins and particulate matter. Immunity 38: 1142–1153. [PubMed: 23809161]

23. Lima H Jr., Jacobson LS, Goldberg MF, Chandran K, Diaz-Griffero F, Lisanti MP, and Brojatsch J. 2013 Role of lysosome rupture in controlling Nlrp3 signaling and necrotic cell death. Cell Cycle 12: 1868–1878. [PubMed: 23708522]

24. Brojatsch J, Lima H, Palliser D, Jacobson LS, Muehlbauer SM, Furtado R, Goldman DL, Lisanti MP, and Chandran K. 2015 Distinct cathepsins control necrotic cell death mediated by pyroptosis inducers and lysosome-destabilizing agents. Cell Cycle 14: 964–972. [PubMed: 25830414]

25. Weissmann G, and Rita GA. 1972 Molecular basis of gouty inflammation: interaction of monosodium urate crystals with lysosomes and liposomes. Nat New Biol 240: 167–172. [PubMed: 4343947]

26. Wallingford WR, and McCarty DJ. 1971 Differential membranolytic effects of microcrystalline sodium urate and calcium pyrophosphate dihydrate. J Exp Med 133: 100–112. [PubMed: 4321912]

27. Dostert C, Guarda G, Romero JF, Menu P, Gross O, Tardivel A, Suva ML, Stehle JC, Kopf M, Stamenkovic I, Corradin G, and Tschopp J. 2009 Malarial hemozoin is a Nalp3 inflammasome activating danger signal. PLoS One 4: e6510. [PubMed: 19652710]

28. Desai J, Foresto-Neto O, Honarpisheh M, Steiger S, Nakazawa D, Popper B, Buhl EM, Boor P, Mulay SR, and Anders HJ. 2017 Particles of different sizes and shapes induce neutrophil necroptosis followed by the release of neutrophil extracellular trap-like chromatin. Scientific reports 7: 15003. [PubMed: 29101355]

29. Desai J, Kumar SV, Mulay SR, Konrad L, Romoli S, Schauer C, Herrmann M, Bilyy R, Muller S, Popper B, Nakazawa D, Weidenbusch M, Thomasova D, Krautwald S, Linkermann A, and Anders HJ. 2016 PMA and crystal-induced neutrophil extracellular trap formation involves RIPK1-RIPK3-MLKL signaling. Eur J Immunol 46: 223–229. [PubMed: 26531064]

30. Mulay SR, Desai J, Kumar SV, Eberhard JN, Thomasova D, Romoli S, Grigorescu M, Kulkarni OP, Popper B, Vielhauer V, Zuchtriegel G, Reichel C, Brasen JH, Romagnani P, Bilyy R, Munoz LE, Herrmann M, Liapis H, Krautwald S, Linkermann A, and Anders HJ. 2016 Cytotoxicity of crystals involves RIPK3-MLKL-mediated necroptosis. Nat Commun 7: 10274. [PubMed: 26817517]

31. Kovacs SB, and Miao EA. 2017 Gasdermins: Effectors of Pyroptosis. Trends Cell Biol 27: 673–684. [PubMed: 28619472]

32. Frank D, and Vince JE. 2019 Pyroptosis versus necroptosis: similarities, differences, and crosstalk. Cell Death Differ 26: 99–114. [PubMed: 30341423]

33. Kuang S, Zheng J, Yang H, Li S, Duan S, Shen Y, Ji C, Gan J, Xu XW, and Li J. 2017 Structure insight of GSDMD reveals the basis of GSDMD autoinhibition in cell pyroptosis. Proc Natl Acad Sci U S A 114: 10642–10647. [PubMed: 28928145]

34. Aglietti RA, Estevez A, Gupta A, Ramirez MG, Liu PS, Kayagaki N, Ciferri C, Dixit VM, and Dueber EC. 2016 GsdmD p30 elicited by caspase-11 during pyroptosis forms pores in membranes. Proc Natl Acad Sci U S A 113: 7858–7863. [PubMed: 27339137]

35. Sborgi L, Ruhl S, Mulvihill E, Pipercevic J, Heilig R, Stahlberg H, Farady CJ, Muller DJ, Broz P, and Hiller S. 2016 GSDMD membrane pore formation constitutes the mechanism of pyroptotic cell death. EMBO J 35: 1766–1778. [PubMed: 27418190]

36. Shi J, Zhao Y, Wang K, Shi X, Wang Y, Huang H, Zhuang Y, Cai T, Wang F, and Shao F. 2015 Cleavage of GSDMD by inflammatory caspases determines pyroptotic cell death. Nature 526: 660–665. [PubMed: 26375003]

37. He WT, Wan H, Hu L, Chen P, Wang X, Huang Z, Yang ZH, Zhong CQ, and Han J. 2015 Gasdermin D is an executor of pyroptosis and required for interleukin-1beta secretion. Cell Res 25: 1285–1298. [PubMed: 26611636]

38. Kayagaki N, Stowe IB, Lee BL, O'Rourke K, Anderson K, Warming S, Cuellar T, Haley B, Roose-Girma M, Phung QT, Liu PS, Lill JR, Li H, Wu J, Kummerfeld S, Zhang J, Lee WP, Snipas SJ, Salvesen GS, Morris LX, Fitzgerald L, Zhang Y, Bertram EM, Goodnow CC, and Dixit VM. 2015 Caspase-11 cleaves gasdermin D for non-canonical inflammasome signalling. Nature 526: 666–671. [PubMed: 26375259]

39. Ding J, Wang K, Liu W, She Y, Sun Q, Shi J, Sun H, Wang DC, and Shao F. 2016 Pore-forming activity and structural autoinhibition of the gasdermin family. Nature 535: 111–116. [PubMed: 27281216]

40. Liu X, Zhang Z, Ruan J, Pan Y, Magupalli VG, Wu H, and Lieberman J. 2016 Inflammasome-activated gasdermin D causes pyroptosis by forming membrane pores. Nature 535: 153–158. [PubMed: 27383986]

41. Kanneganti A, Malireddi RKS, Saavedra PHV, Vande Walle L, Van Gorp H, Kambara H, Tillman H, Vogel P, Luo HR, Xavier RJ, Chi H, and Lamkanfi M. 2018 GSDMD is critical for

autoinflammatory pathology in a mouse model of Familial Mediterranean Fever. J Exp Med 215: 1519–1529. [PubMed: 29793924]

42. Xiao J, Wang C, Yao JC, Alippe Y, Xu C, Kress D, Civitelli R, Abu-Amer Y, Kanneganti TD, Link DC, and Mbalaviele G. 2018 Gasdermin D mediates the pathogenesis of neonatal-onset multisystem inflammatory disease in mice. PLoS Biol 16: e3000047. [PubMed: 30388107]

43. Rathkey JK, Zhao J, Liu Z, Chen Y, Yang J, Kondolf HC, Benson BL, Chirieleison SM, Huang AY, Dubyak GR, Xiao TS, Li X, and Abbott DW. 2018 Chemical disruption of the pyroptotic pore-forming protein gasdermin D inhibits inflammatory cell death and sepsis. Sci Immunol 3: eaat2738 [PubMed: 30143556]

44. Sollberger G, Choidas A, Burn GL, Habenberger P, Di Lucrezia R, Kordes S, Menninger S, Eickhoff J, Nussbaumer P, Klebl B, Kruger R, Herzig A, and Zychlinsky A. 2018 Gasdermin D plays a vital role in the generation of neutrophil extracellular traps. Sci Immunol 3: eaar6689 [PubMed: 30143555]

45. Monteleone M, Stanley AC, Chen KW, Brown DL, Bezbradica JS, von Pein JB, Holley CL, Boucher D, Shakespear MR, Kapetanovic R, Rolfes V, Sweet MJ, Stow JL, and Schroder K. 2018 Interleukin-1beta Maturation Triggers Its Relocation to the Plasma Membrane for Gasdermin-D-Dependent and -Independent Secretion. Cell Rep 24: 1425–1433. [PubMed: 30089254]

46. Schneider KS, Gross CJ, Dreier RF, Saller BS, Mishra R, Gorka O, Heilig R, Meunier E, Dick MS, Cikovic T, Sodenkamp J, Medard G, Naumann R, Ruland J, Kuster B, Broz P, and Gross O. 2017 The Inflammasome Drives GSDMD-Independent Secondary Pyroptosis and IL-1 Release in the Absence of Caspase-1 Protease Activity. Cell Rep 21: 3846–3859. [PubMed: 29281832]

47. Conos SA, Lawlor KE, Vaux DL, Vince JE, and Lindqvist LM. 2016 Cell death is not essential for caspase-1-mediated interleukin-1beta activation and secretion. Cell Death Differ 23: 1827–1838. [PubMed: 27419363]

48. Evavold CL, Ruan J, Tan Y, Xia S, Wu H, and Kagan JC. 2018 The Pore-Forming Protein Gasdermin D Regulates Interleukin-1 Secretion from Living Macrophages. Immunity 48: 35–44 e36. [PubMed: 29195811]

49. Sun L, Wang H, Wang Z, He S, Chen S, Liao D, Wang L, Yan J, Liu W, Lei X, and Wang X. 2012 Mixed lineage kinase domain-like protein mediates necrosis signaling downstream of RIP3 kinase. Cell 148: 213–227. [PubMed: 22265413]

50. Conos SA, Chen KW, De Nardo D, Hara H, Whitehead L, Nunez G, Masters SL, Murphy JM, Schroder K, Vaux DL, Lawlor KE, Lindqvist LM, and Vince JE. 2017 Active MLKL triggers the NLRP3 inflammasome in a cell-intrinsic manner. Proc Natl Acad Sci U S A 114: E961–E969. [PubMed: 28096356]

51. Honarpisheh M, Foresto-Neto O, Desai J, Steiger S, Gomez LA, Popper B, Boor P, Anders HJ, and Mulay SR. 2017 Phagocytosis of environmental or metabolic crystalline particles induces cytotoxicity by triggering necroptosis across a broad range of particle size and shape. Scientific reports 7: 15523. [PubMed: 29138474]

52. Cullen SP, Kearney CJ, Clancy DM, and Martin SJ. 2015 Diverse Activators of the NLRP3 Inflammasome Promote IL-1beta Secretion by Triggering Necrosis. Cell Rep 11: 1535–1548. [PubMed: 26027935]

53. Weinberg JM, Bienholz A, and Venkatachalam MA. 2016 The role of glycine in regulated cell death. Cell Mol Life Sci 73: 2285–2308. [PubMed: 27066896]

54. Franklin BS, Mangan MS, and Latz E. 2016 Crystal Formation in Inflammation. Annu Rev Immunol 34: 173–202. [PubMed: 26772211]

55. Xu C, Lu Z, Luo Y, Liu Y, Cao Z, Shen S, Li H, Liu J, Chen K, Chen Z, Yang X, Gu Z, and Wang J. 2018 Targeting of NLRP3 inflammasome with gene editing for the amelioration of inflammatory diseases. Nat Commun 9: 4092. [PubMed: 30291237]

56. Joosten LA, Netea MG, Mylona E, Koenders MI, Malireddi RK, Oosting M, Stienstra R, van de Veerdonk FL, Stalenhoef AF, Giamarellos-Bourboulis EJ, Kanneganti TD, and van der Meer JW. 2010 Engagement of fatty acids with Toll-like receptor 2 drives interleukin-1beta production via the ASC/caspase 1 pathway in monosodium urate monohydrate crystal-induced gouty arthritis. Arthritis Rheum 62: 3237–3248. [PubMed: 20662061]

57. Joosten LA, Ea HK, Netea MG, and Busso N. 2011 Interleukin-1beta activation during acute joint inflammation: A limited role for the NLRP3 inflammasome in vivo. Joint Bone Spine 78: 107–110. [PubMed: 21183380]

58. Guma M, Ronacher L, Liu-Bryan R, Takai S, Karin M, and Corr M. 2009 Caspase 1-independent activation of interleukin-1beta in neutrophil-predominant inflammation. Arthritis Rheum 60: 3642–3650. [PubMed: 19950258]

59. Hoffman HM, Scott P, Mueller JL, Misaghi A, Stevens S, Yancopoulos GD, Murphy A, Valenzuela DM, and Liu-Bryan R. 2010 Role of the leucine-rich repeat domain of cryopyrin/NALP3 in monosodium urate crystal-induced inflammation in mice. Arthritis Rheum 62: 2170–2179. [PubMed: 20506351]

60. Shu F, Chen J, Ma X, Fan Y, Yu L, Zheng W, Amrein MW, Xia T, and Shi Y. 2018 Cholesterol Crystal-Mediated Inflammation Is Driven by Plasma Membrane Destabilization. Front Immunol 9: 1163. [PubMed: 29896195]

61. Vince JE, De Nardo D, Gao W, Vince AJ, Hall C, McArthur K, Simpson D, Vijayaraj S, Lindqvist LM, Bouillet P, Rizzacasa MA, Man SM, Silke J, Masters SL, Lessene G, Huang DCS, Gray DHD, Kile BT, Shao F, and Lawlor KE. 2018 The Mitochondrial Apoptotic Effectors BAX/BAK Activate Caspase-3 and −7 to Trigger NLRP3 Inflammasome and Caspase-8 Driven IL-1beta Activation. Cell Rep 25: 2339–2353 e2334. [PubMed: 30485804]

62. Gutierrez KD, Davis MA, Daniels BP, Olsen TM, Ralli-Jain P, Tait SW, Gale M Jr., and Oberst A. 2017 MLKL Activation Triggers NLRP3-Mediated Processing and Release of IL-1beta Independently of Gasdermin-D. J Immunol 198: 2156–2164. [PubMed: 28130493]

63. Chatfield SM, Grebe K, Whitehead LW, Rogers KL, Nebl T, Murphy JM, and Wicks IP. 2018 Monosodium Urate Crystals Generate Nuclease-Resistant Neutrophil Extracellular Traps via a Distinct Molecular Pathway. J Immunol 200: 1802–1816. [PubMed: 29367211]

64. Fink SL, and Cookson BT. 2006 Caspase-1-dependent pore formation during pyroptosis leads to osmotic lysis of infected host macrophages. Cell Microbiol 8: 1812–1825. [PubMed: 16824040]

65. Verhoef PA, Kertesy SB, Lundberg K, Kahlenberg JM, and Dubyak GR. 2005 Inhibitory effects of chloride on the activation of caspase-1, IL-1beta secretion, and cytolysis by the P2X7 receptor. J Immunol. 175: 7623–7634. [PubMed: 16301672]

66. Mihalik R, Imre G, Petak I, Szende B, and Kopper L. 2004 Cathepsin B-independent abrogation of cell death by CA-074-OMe upstream of lysosomal breakdown. Cell Death Differ 11: 1357–1360. [PubMed: 15297886]

67. Bogyo M, Verhelst S, Bellingard-Dubouchaud V, Toba S, and Greenbaum D. 2000 Selective targeting of lysosomal cysteine proteases with radiolabeled electrophilic substrate analogs. Chem Biol 7: 27–38. [PubMed: 10662686]

68. Vanden Berghe T, Vanlangenakker N, Parthoens E, Deckers W, Devos M, Festjens N, Guerin CJ, Brunk UT, Declercq W, and Vandenabeele P. 2010 Necroptosis, necrosis and secondary necrosis converge on similar cellular disintegration features. Cell Death Differ 17: 922–930. [PubMed: 20010783]

69. Foghsgaard L, Wissing D, Mauch D, Lademann U, Bastholm L, Boes M, Elling F, Leist M, and Jaattela M. 2001 Cathepsin B acts as a dominant execution protease in tumor cell apoptosis induced by tumor necrosis factor. J Cell Biol 153: 999–1010. [PubMed: 11381085]

70. Hentze H, Lin XY, Choi MS, and Porter AG. 2003 Critical role for cathepsin B in mediating caspase-1-dependent interleukin-18 maturation and caspase-1-independent necrosis triggered by the microbial toxin nigericin. Cell Death Differ 10: 956–968. [PubMed: 12934070]

71. Ekert PG, Read SH, Silke J, Marsden VS, Kaufmann H, Hawkins CJ, Gerl R, Kumar S, and Vaux DL. 2004 Apaf-1 and caspase-9 accelerate apoptosis, but do not determine whether factor-deprived or drug-treated cells die. J Cell Biol 165: 835–842. [PubMed: 15210730]

72. Marsden VS, O'Connor L, O'Reilly LA, Silke J, Metcalf D, Ekert PG, Huang DC, Cecconi F, Kuida K, Tomaselli KJ, Roy S, Nicholson DW, Vaux DL, Bouillet P, Adams JM, and Strasser A. 2002 Apoptosis initiated by Bcl-2-regulated caspase activation independently of the cytochrome c/Apaf-1/caspase-9 apoptosome. Nature 419: 634–637. [PubMed: 12374983]

73. Flach TL, Ng G, Hari A, Desrosiers MD, Zhang P, Ward SM, Seamone ME, Vilaysane A, Mucsi AD, Fong Y, Prenner E, Ling CC, Tschopp J, Muruve DA, Amrein MW, and Shi Y. 2011 Alum

interaction with dendritic cell membrane lipids is essential for its adjuvanticity. Nat Med 17: 479–487. [PubMed: 21399646]

74. Murphy JM, Czabotar PE, Hildebrand JM, Lucet IS, Zhang JG, Alvarez-Diaz S, Lewis R, Lalaoui N, Metcalf D, Webb AI, Young SN, Varghese LN, Tannahill GM, Hatchell EC, Majewski IJ, Okamoto T, Dobson RC, Hilton DJ, Babon JJ, Nicola NA, Strasser A, Silke J, and Alexander WS. 2013 The Pseudokinase MLKL Mediates Necroptosis via a Molecular Switch Mechanism. Immunity 39: 443–453. [PubMed: 24012422]

75. Ortiz-Bravo E, Sieck MS, and Schumacher HR Jr. 1993 Changes in the proteins coating monosodium urate crystals during active and subsiding inflammation. Immunogold studies of synovial fluid from patients with gout and of fluid obtained using the rat subcutaneous air pouch model. Arthritis Rheum 36: 1274–1285. [PubMed: 8216421]

76. Kuida K, Lippke JA, Ku G, Harding MW, Livingston DJ, Su MS, and Flavell RA. 1995 Altered cytokine export and apoptosis in mice deficient in interleukin-1 beta converting enzyme. Science 267: 2000–2003. [PubMed: 7535475]

Key Points:

- MSU crystals and alum rapidly activate GSDMD

- GSDMD is dispensable for MSU crystal- and alum-induced IL-1β release and cell death

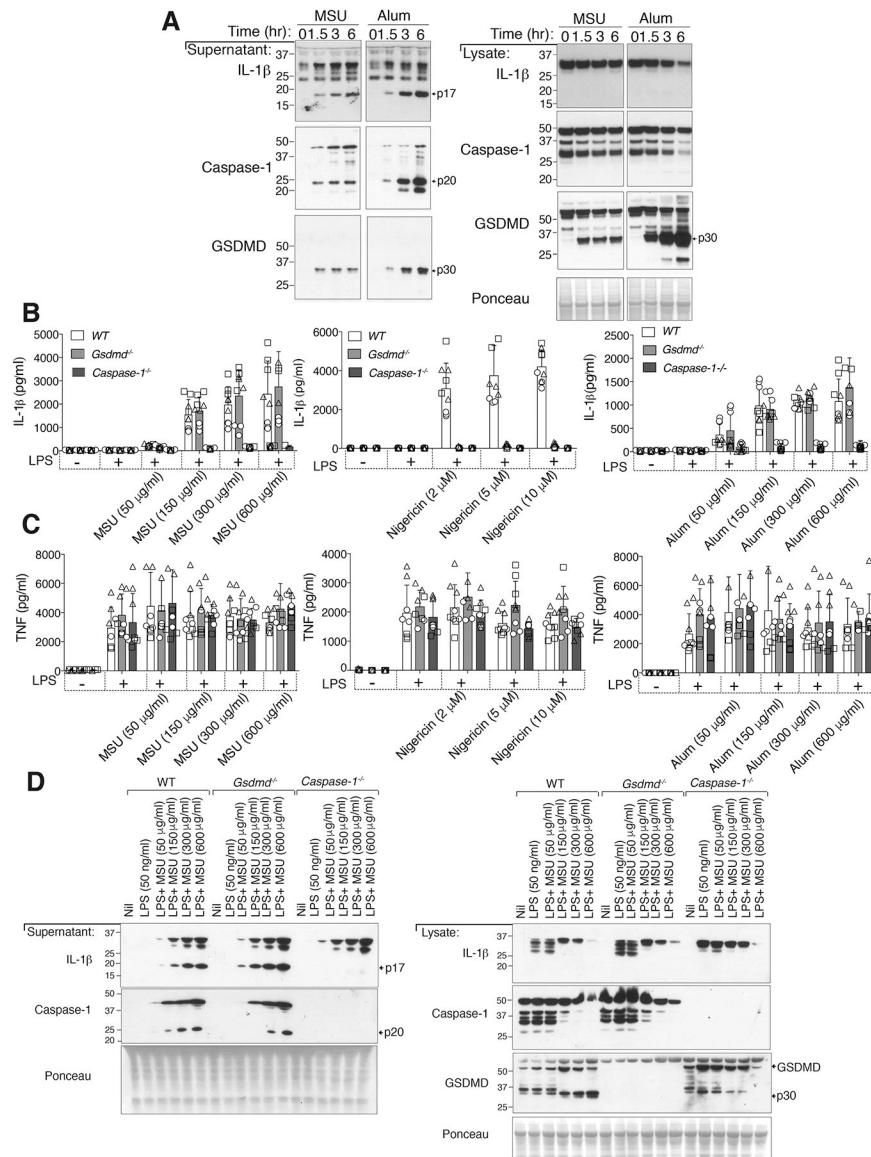- Cathepsins, caspases and MLKL are not required for MSU crystal-induced cell killing

Figure 1. MSU crystals and alum activate IL-1β and GSDMD, but GSDMD is dispensable for IL-1β release.

(A) Bone marrow-derived macrophages (BMDMs) from WT (C57BL/6) mice were pre-incubated for 2.5 hr with LPS (50 ng/ml) and then treated with MSU crystals or alum (300 µg/ml) for the indicated times. Cell supernatant and total cell lysates were analyzed by immunoblot. Ponceau stain depicts protein loading. **(B)** IL-1β and **(C)** TNF levels in the cell supernatant of BMDMs from WT (C57BL/6), $Gsdmd^{-/-}$ and $Caspase\text{-}1^{-/-}$ mice pre-incubated for 2.5 hr with LPS (50 ng/ml) and then treated with the indicated concentrations of MSU crystals (6 hr), nigericin (1 hr) and alum (6 hr). **(D)** BMDMs from WT (C57BL/6), $Gsdmd^{-/-}$ and $Caspase\text{-}1^{-/-}$ mice were pre-incubated with LPS (50 ng/ml, 2.5 hr) and then treated with the indicated concentrations of MSU crystals (6 hr) and the cell supernatant and total cell lysates analyzed by immunoblot. Ponceau staining depicts protein loading. (B and C) Mean ± SD of 7–9 replicates pooled from three independent experiments (symbols). (A and D) One of two independent experiments.
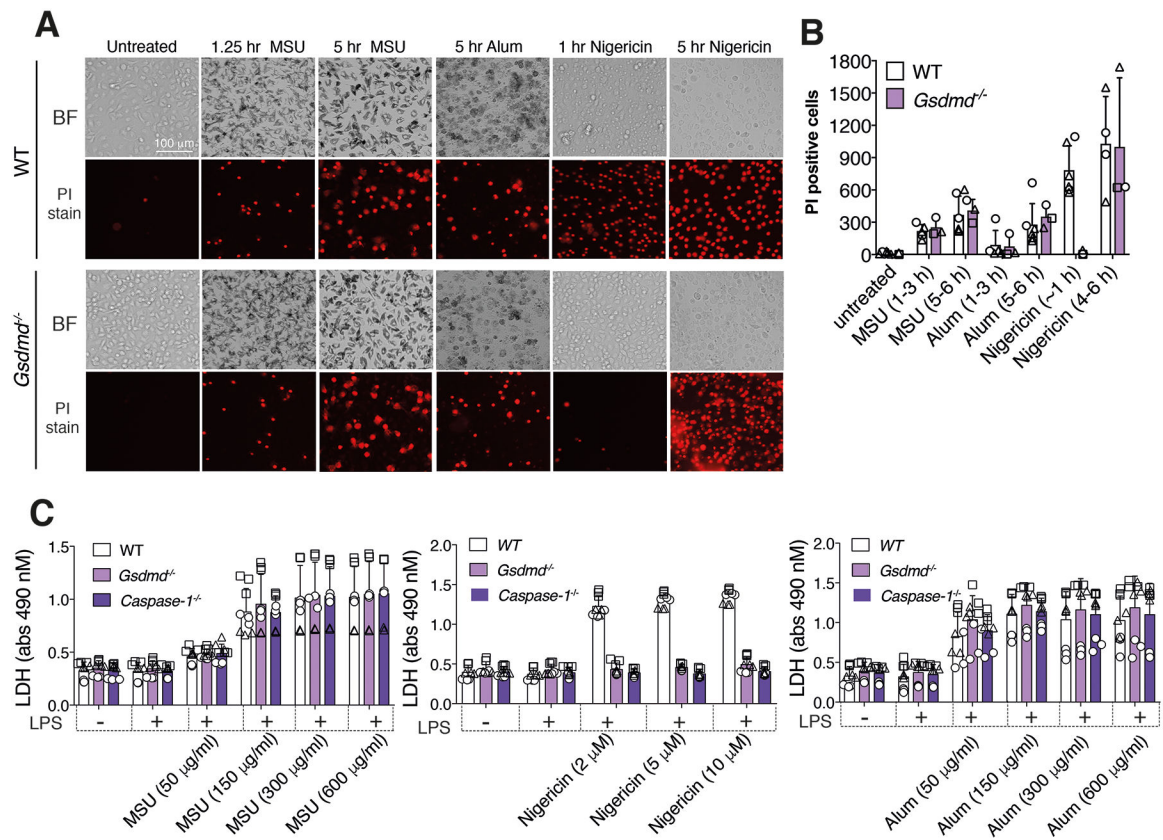
Figure 2. GSDMD is not required for MSU crystal- and alum-induced cell death.
(A and B) Imaging of BMDMs from WT and *Gsdmd*^{−/−} mice pre-incubated for 2.5 hr with LPS (50 ng/ml) and then treated with MSU crystals (300 μg/ml), nigericin (10 μM) or alum (300 μg/ml) for the indicated times. Cell death was assessed by propidium iodide (PI) uptake (red fluorescence). Representative bright field (BF) and PI images are shown in (A) and the number of PI positive cells from three independent experiments (symbols) quantified (mean ± SD) in (B) using Fiji imaging software. **(C)** LDH levels in the cell supernatant of BMDMs from WT (C57BL/6), *Gsdmd*^{−/−} and *Caspase*-1^{−/−} mice pre-incubated with LPS (50 ng/ml, 2.5 hr) and then treated with the indicated concentrations of MSU crystals (6 hr) or nigericin (1 hr). Mean ± SD of 9 replicates (symbols) pooled from three independent experiments.
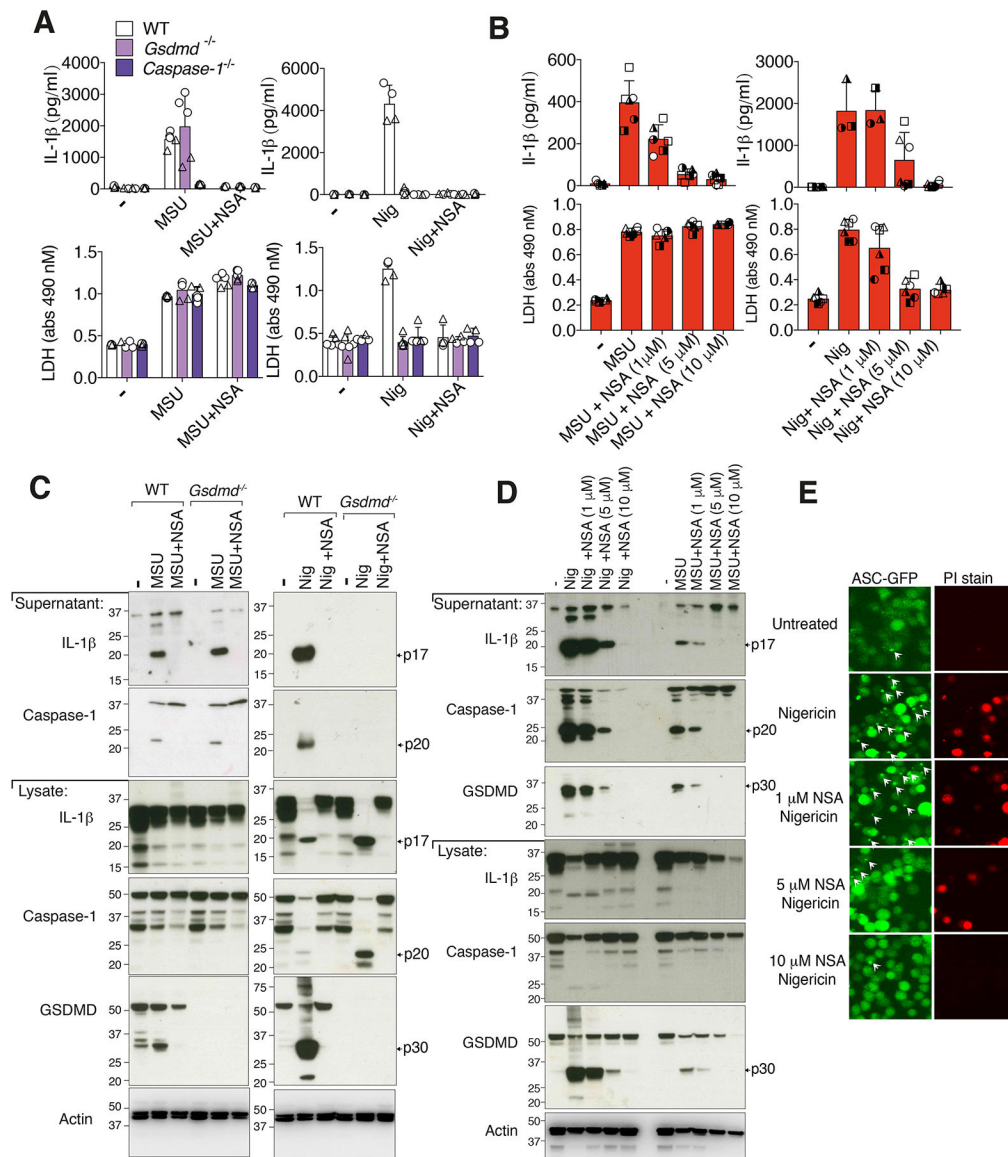
Figure 3. Necrosulfonamide inhibits NLRP3 activation and pyroptosis independent of GSDMD targeting.
(**A**) IL-1β (top panel) and LDH (bottom panel) levels in the cell supernantant of BMDMs from WT (C57BL/6), *Gsdmd*^{−/−} and *Caspase-1*^{−/−} mice primed for 2.5 hr with LPS (50 ng/ ml), with necrosulfonamide (NSA) (10 μM) added in the last 30 min of priming, then treated with MSU crystals (300 μg/ml, 6 hr) or nigericin (10 μM, 1 hr). (**B**) IL-1β and LDH levels in the supernatant of BMDMs from WT (C57BL/6) mice primed with LPS (50 ng/ml, 2.5 hr), with the indicated concentration of NSA added in the last 30 min of priming, followed by treatment with MSU crystals (300 μg/ml, 6 hr) or nigericin (10 μM, 1 hr). (**C**) WT (C57BL/6) and *Gsdmd*^{−/−} BMDMs were treated as in (A) and supernatant and total cell lysates analyzed by immunoblot. (**D**) WT (C57BL/6) BMDMs were treated as in (B) and supernatant and total cell lysates analyzed by immunoblot. Ponceau staining depicts protein loading. (**E**) Immortalized BMDMs (iBMDMs) expressing ASC-GFP and FLAG-NLRP3 were analyzed by fluorescent microscopy for ASC speck formation (green fluorescence) and

PI uptake (red fluorescence) after treatment with the indicated concentrations of NSA for 30–40 min and then nigericin (10 μM, 80 min). ASC specks are indicated with white arrows. (A) Mean ± SD of 4–5 replicates (symbols) pooled from two independent experiments. (B) Mean ± SD of BMDMs from 3–6 mice (symbols) pooled from two independent experiments. (C, D and E) Data are representative of three independent experiments.
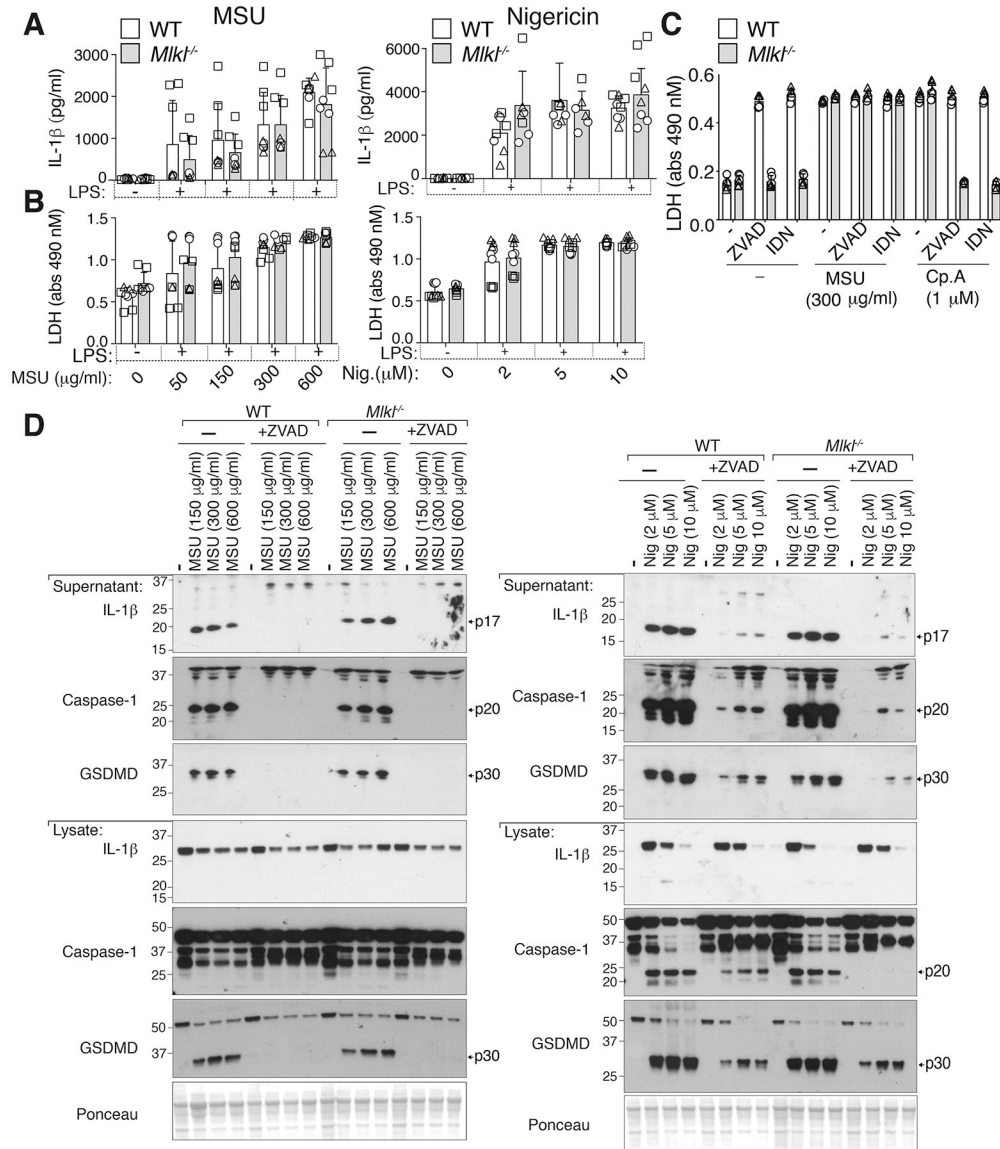
Figure 4. MLKL is not required for MSU crystal-induced death or NLRP3 inflammasome activation in macrophages.

(A) IL-1β and (B) LDH levels in the cell supernatant of BMDMs from WT (C57BL/6) and *Mlkl*^{−/−} mice primed with LPS (50 ng/ml, 2.5 hr) and then treated with the indicated concentrations of MSU crystals (6 hr) or nigericin (1 hr). (C) LDH levels in the cell supernatant of BMDMs from WT (C57BL/6) and *Mlkl*^{−/−} mice primed with LPS (50 ng/ml, 2.5 hr), with Z-VAD-fmk (40 μM) or IDN-6556 (20 μM) added in the last 30 min of priming, then treated with MSU crystals (300 μg/ml or Smac-mimetic compound (Cp.A, 1 μM) for 6 hr (D) BMDMs from WT (C57BL/6) and *Mlkl*^{−/−} mice primed with LPS (50 ng/ml, 2.5 hr), with Z-VAD-fmk (20 μM) added in the last 30 min of priming, were then treated with the indicated concentrations of MSU crystals (6 hr) or nigericin (1 hr). Cell supernatants and total cell lysates were analyzed by immunoblot, as indicated. Ponceau staining depicts protein loading. (A, B, C) Mean ± SD of 8 (A, B) or 6 (C) replicates pooled

from three (A, B) or two (C) independent experiments. (D) Data are representative of two independent experiments.
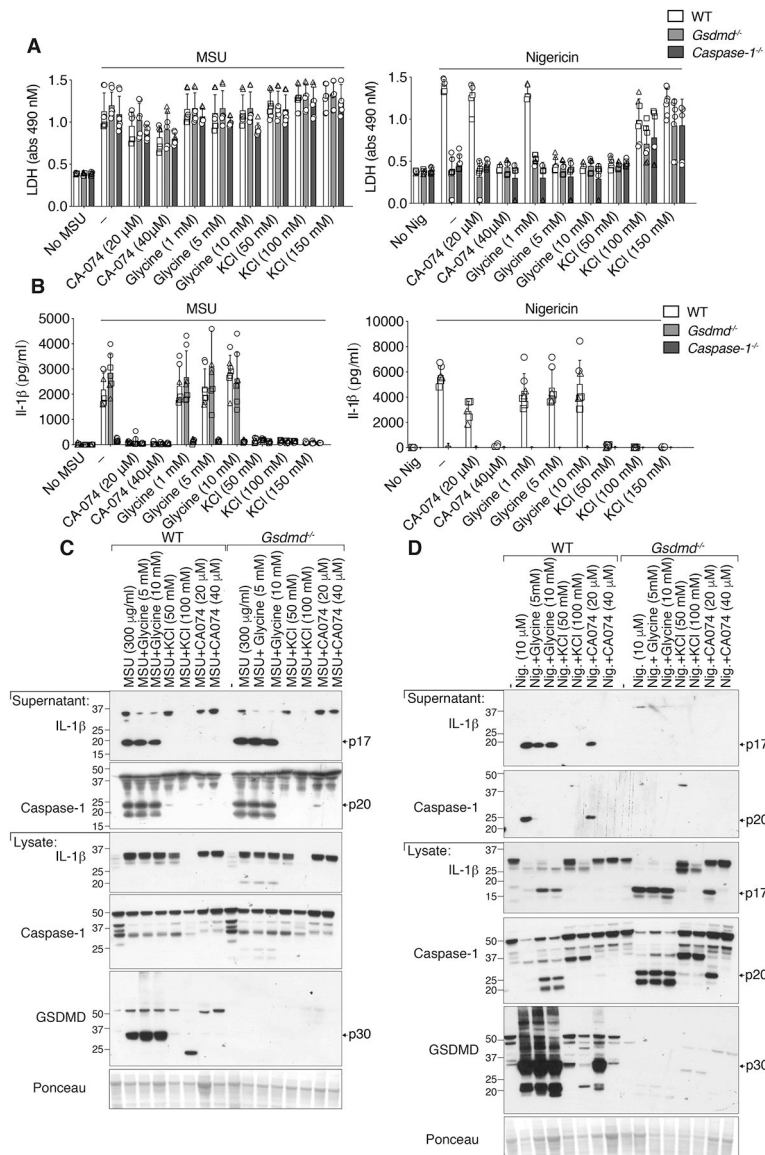
Figure 5. MSU crystal-induced membrane lysis is not significantly reduced by the osmoprotectant glycine, the prevention of potassium ion efflux, or the inhibition of cathepsin activity.

(**A**) LDH and (**B**) IL-1β levels in the cell supernatant of BMDMs from WT (C57BL/6), *Gsdmd*^{−/−} and *Caspase-1*^{−/−} mice primed with LPS (50 ng/ml, 2.5 hr), with the indicated concentrations of CA-074-Me, glycine and potassium chloride (KCl) added in the last 30 min of priming, and then treated with MSU crystals (300 μg/ml, 6 hr) or nigericin (10 μM, 1 hr). (**C and D**) BMDMs from WT (C57BL/6) and *Gsdmd*^{−/−} mice were treated as (A) and cell supernatant and total cell lysates analyzed by immunoblot, as indicated. Ponceau staining depicts protein loading. (A, B) Mean ± SD of 7–9 replicates pooled from three independent experiments. (C, D) Data representative of two independent experiments.
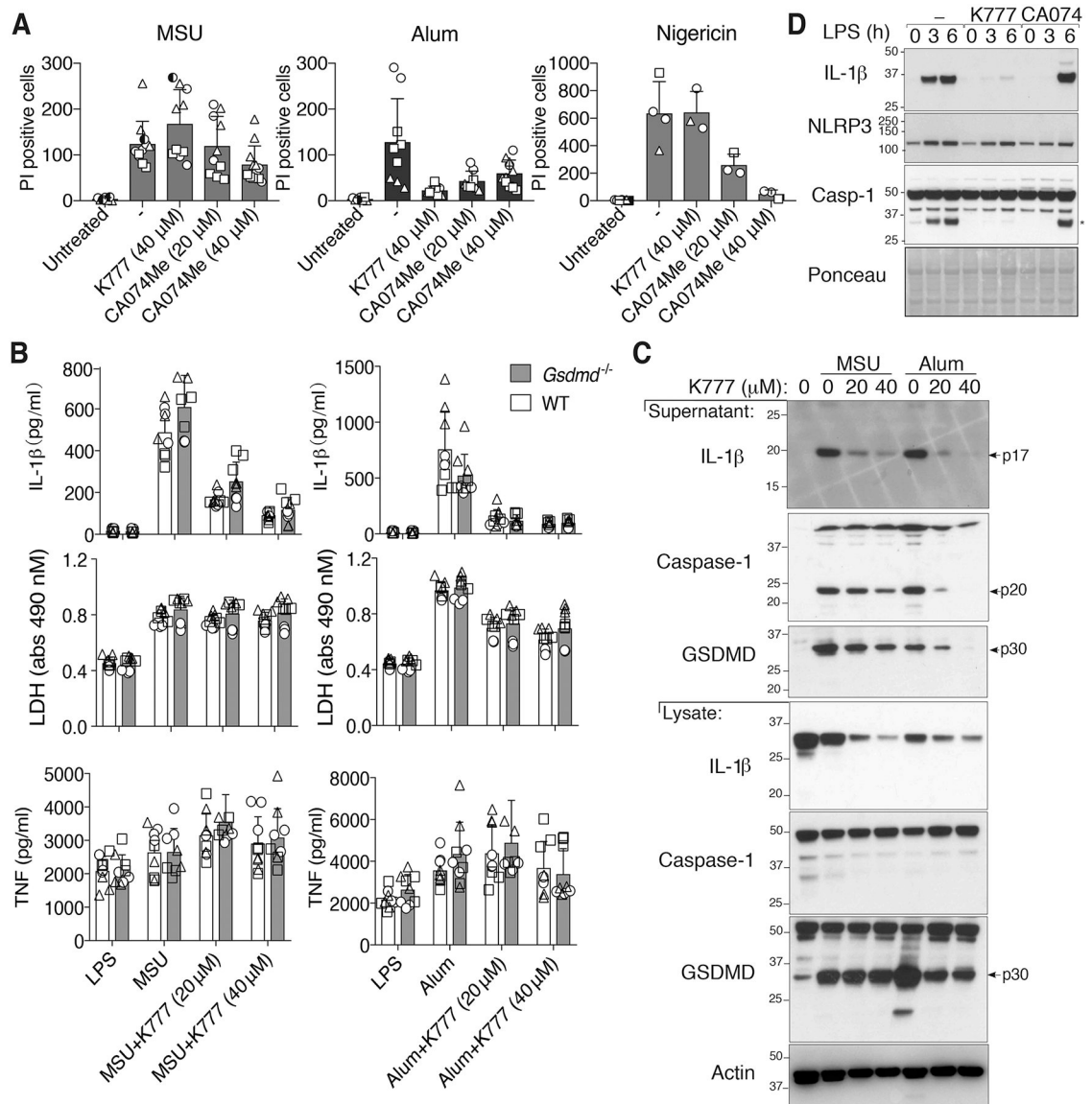
Figure 6. The cathepsin inhibitors, K777 and CA-074-Me, do not prevent MSU crystal-induced death but do reduce inflammasome priming.

(**A**) BMDMs pre-treated with the indicated cathepsin inhibitors for 40–60 min were then stimulated with MSU (300 μg/ml), alum (300 μg/ml) or nigericin (10 μM) for 4–5 hrs, stained with propidium iodide (PI), and imaged. PI uptake was quantified using Fiji. See Figure S4 for representative images. (**B**) BMDMs from WT and *Gsdmd*^{−/−} mice primed with LPS (50 ng/ml, 2.5 hr), and treated in the last 30 min with K777 (20 μM or 40 μM), were then stimulated with MSU (300 μg/ml) or alum (300 μg/ml) for 6 hr. Levels of IL-1β, TNF and LDH in the cell supernatant were measured. (**C**) BMDMs were treated as in (B) and cell supernatant and total cell lysates analyzed by immunoblot. (**D**) BMDMs were pre-treated with the indicated cathepsin inhibitor (40 μM) for 40–60 min then stimulated with LPS (100 ng/ml) and total cell lysates examined by immunoblot. *IL-1β band. (A) Mean ± SD of two (nigericin) or three (MSU and alum) pooled independent experiments. Similar symbols represent multiple images per experiment. Different symbols represent independent

experiments. (B) Mean ± SD of 6–9 replicates (symbols) pooled from three independent experiments. (C and D) Data are representative of two (C) or three (D) independent experiments.
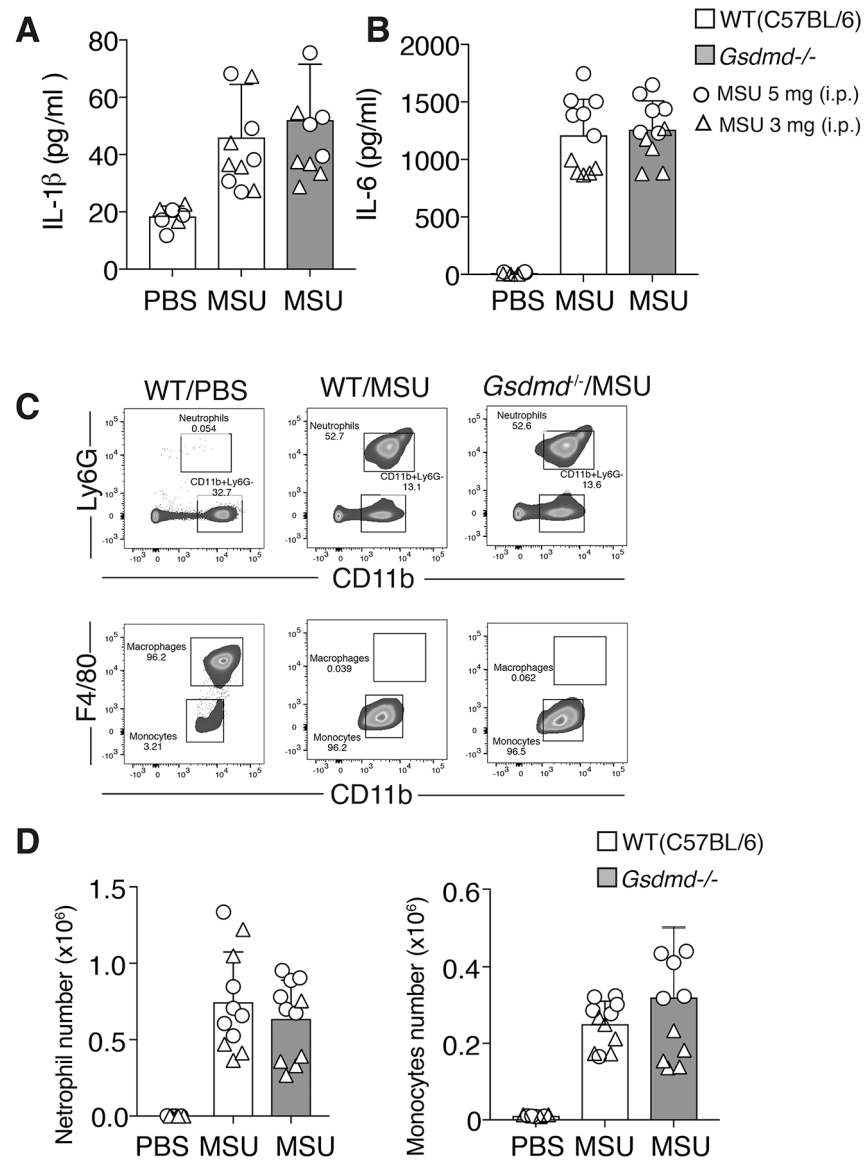
Figure 7. GSDMD is dispensable for MSU crystal-induced IL-1β release and neutrophil and monocyte influx *in vivo*.

C57BL/6 and *Gsdmd*^−/−^ mice were injected i.p. with carrier (PBS) or MSU crystals (3 mg [triangles] or 5 mg [circles]) and **(A)** IL-1β and **(B)** IL-6 levels measured in the peritoneal lavage fluid supernatant after 4 hr. **(C)** Gating strategy for neutrophil and monocyte quantification in peritoneal lavage fluid. **(D)** Quantification of peritoneal influx of neutrophils and monocytes in C57BL/6 and *Gsdmd*^−/−^ mice i.p. injected with carrier (PBS) or MSU crystals (3 mg [triangles] or 5 mg [circles]) for 4 hr (A, B and D) Mean ± SD, n=11 mice per group (symbols) pooled from two independent experiments.